

Perfusion-Guided Monitoring of Tumor Response to Sonoporation and Prediction of Liposomal Doxorubicin Uptake Using Microbubble Contrast Agents

Aditi Bellary¹, Arelly Villarreal¹, Rojin Eslami¹, Quincy Undseth¹, Sonia Hernandez², Bianca Lec²,
Jessica Kandel², Mark Borden³, Sumbul Shaikh⁴, Rajiv Chopra⁴, Shashank Sirsi^{1,4}

¹Department of Biomedical Engineering, University of Texas at Dallas, Richardson, TX.

²Department of Surgery, University of Chicago Medical School, Chicago, IL.

³Department of Mechanical Engineering, University of Colorado at Boulder, Boulder, CO.

⁴Department of Radiology, University of Texas Southwestern Medical Center, Dallas, TX.

Abstract—Microbubble ultrasound contrast agents (UCAs) are frequently used for *in vivo* imaging applications to evaluate changes in tumor perfusion using quantitative contrast enhanced ultrasound (qCEUS) imaging. In addition, volumetric oscillation of these microbubbles in an acoustic field can promote drug extravasation into tumor tissue by permeabilizing cell membranes by a technique known as sonoporation. In this study, we propose that qCEUS imaging can be used to effectively monitor the efficacy of sonoporation *in vivo*. Importantly, we demonstrate that changes in microbubble perfusion kinetics can function as effective predictors of sonoporation efficiency *in vivo*. However, the overall degree of tumor perfusion – which is not altered by sonoporation – correlates strongly with drug uptake. Our results suggest that qCEUS can be harnessed to provide real-time feedback detailing vascular changes that occur during sonoporation, and that these biologically driven phenomena can be correlated with nanoparticle uptake in tumors. Successful implementation of this strategy could lead to improved methods of monitoring tumor response to therapy in the clinic, thus furthering strides toward the goal of more personalized therapies.

Keywords—Ultrasound contrast agents (microbubbles); CEUS; image guided drug delivery; personalized medicine

I. INTRODUCTION

Nanomedicine employs carrier vehicles with sizes in the range of 1-100 nm to passively target tumors via the Enhanced Permeability and Retention (EPR) effect [1]. The EPR effect is largely attributed to the leakiness of the tumor vasculature, which in turn allows nanomaterials to circulate for prolonged periods – avoiding clearance by the reticuloendothelial (RES) system – and to gradually amass in the tumor [2]. Although effective, the EPR effect is highly variable, and numerous studies have established the EPR effect to be dependent on cancer type and stage [3]; a low

EPR environment has been proven to impede drug transport [4-6]. Given this reality, novel strategies hinging on active targeting must be pursued to augment intratumoral accumulation of chemotherapeutic agents.

Microbubble contrast agents are responsive to ultrasound and can be utilized for the purpose of imaging as well as site-specific delivery of its enclosed gas, or any drug/molecule that is tethered to it. These microbubbles are gas-filled spheres that are 1 to 10 μm in diameter and are composed of a stabilized lipid shell. The compressibility of the microbubble gas core allows it to expand and contract in response to pressure changes associated with an acoustic sound wave. At low-pressure amplitudes, the microbubble oscillates volumetrically and can exert shear forces on cells in its vicinity to promote passive uptake via endocytosis [7]. At high-pressure amplitudes, the microbubble collapses and emits shock waves that can create pores in cell membranes, thus increasing permeability to circulating therapeutic agents [8]. This phenomenon is known as sonoporation, as it combines ultrasound and microbubbles, and can be exploited to improve extravasation of drugs or nanoparticles – by judiciously applying focused ultrasound, the effects of sonoporation can be spatially and temporally controlled to improve localized drug deposition [9-10].

While the concept of sonoporation has been studied for over two decades (predominantly *in vitro*), the delivery of conventional nanomedicines – namely liposomal doxorubicin – *in vivo* is more limited. In one of the more relevant studies which used fluorescent liposomes as a surrogate for L-DOX, Theek *et al* showed that sonoporation could improve intratumoral liposomal penetration, even in tumor models characterized by extensive stromal compartments and dense collagen networks [11]. Tinkov *et*

This work was supported in part by the NCI and NIBIB (NIH grant numbers R01 CA235756 01A1 and 1R21EB015040 01A1 respectively).

illustrated that sonoporation caused preferential uptake of doxorubicin in tumors, citing a 12-fold increase in intratumoral doxorubicin concentration following sonoporation [12]. The majority of these studies used microscopy and tissue extraction procedures to quantify drug accumulation and relied upon physical measurements made with calipers to plot tumor growth and animal survival curves [13]. But a major deficiency in this field of research is that *ex vivo* analysis currently serves as the only method to quantify drug uptake. In the context of ultrasound-triggered microbubble destruction (UTMD), passive cavitation detection is being investigated as a technique to calculate stable and inertial cavitation doses [14]. This technique is useful for monitoring energy generated by bubbles during cavitation, but it does not consider the bioeffects of sonoporation on the tumor vasculature. To address this limitation, we developed a highly controlled method to examine the effects of sonoporation *in vivo* using qCEUS imaging to gauge changes in blood volume and perfusion kinetics. Our study demonstrates that (1) sonoporation efficiently increases liposomal doxorubicin (L-DOX) uptake in tumors and (2) monitoring of the effects of tumor vasculature can be accomplished simultaneously with sonoporation. Moreover, our results strongly suggest that perfusion changes can be effective predictors of sonoporation efficiency *in vivo*.

II. MATERIALS AND METHODS

A. Preparation of Microbubbles

Microbubbles were formulated using a lipid film composed of 14.34 mg of DSPC and 5.66 mg of DSPE-PEG2000, dissolved in chloroform. The lipid solution was evaporated for 48 hours and then stored as lipid films in

sealed scintillation vials at $-20\text{ }^{\circ}\text{C}$. On the day of intended use, the 20-mg film was diluted to 2 mg/mL in a filtered pH 7.5, 10 % propylene glycol (v/v) and 10 % glycerol (v/v) PBS solution. The lipid solution was heated to $65\text{ }^{\circ}\text{C}$ and bath sonicated until the lipid was completely suspended. Microbubbles were generated using probe micro-tip sonication at 70% power under constant flushing with PFB for 10 seconds. The amalgamated lipid suspension was brought below the glass phase temperature and washed three times in a 10 mL Luer tip syringe at 300g for 3 minutes, until the infranatant appeared clear. The microbubbles were characterized using a Multisizer 4e Coulter Counter (MS4) to determine size distribution and concentration.

B. Liposome Formulation

A mock Doxil micelle was fabricated using a lipid film containing 7.56 mg of DSPC, 2.69 mg of cholesterol, and 2.44 of DSPE-PEG2K. The lipid solution was evaporated for 48 hours and then stored as lipid films in sealed scintillation vials at $-20\text{ }^{\circ}\text{C}$. On the day of intended use, the 10-mg film was diluted to 8 mg/mL with filtered pH 7.5 PBS and heated to $65\text{ }^{\circ}\text{C}$ via bath sonication until the lipid became fully suspended. For the purpose of fluorescence microscopy, DiD was added to the liposome solution at $2.1\text{ }\mu\text{g}$ per 1 mg of lipid and sonicated an additional 10 min.

C. Matrigel and Tumor Implantations

Matrigel plugs (BD Biosciences, Franklin Lakes, NJ) mixed with $1\text{ }\mu\text{g}$ basic fibroblast growth factor (Sigma Aldrich, St. Lois, MO) and heparin (Sigma Aldrich) were injected subcutaneously into 6-8 week old CD-1 mice (Charles River, Wilmington, MA). Contrast enhanced ultrasound imaging was performed at 10-14 days.

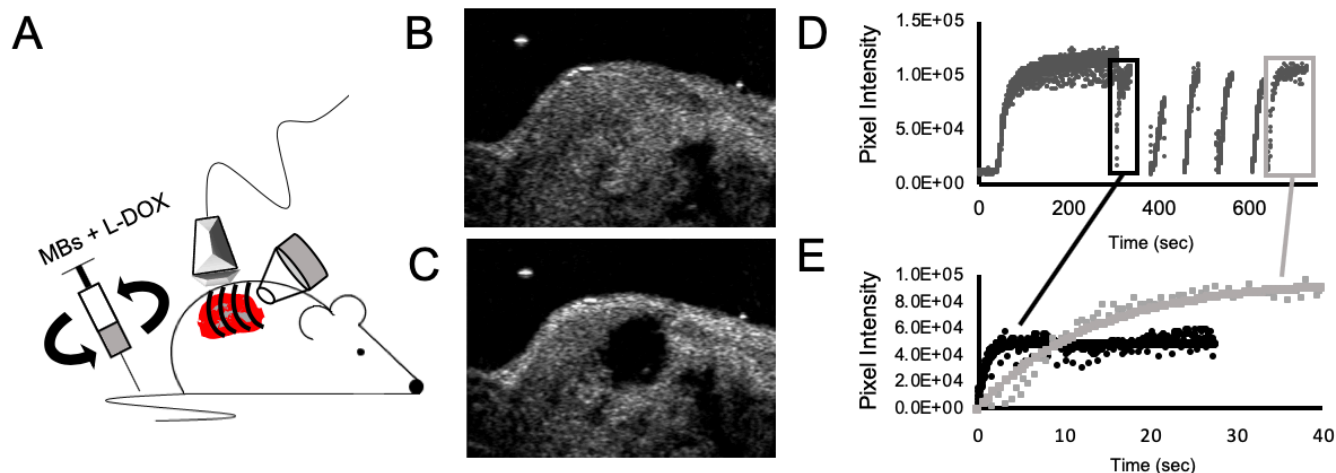


Fig. 1. Perfusion-guided imaging of tumors using qCEUS to monitor sonoporation effects on the vasculature. (A) A rotating syringe pump was developed to administer constant infusions over long periods of time. Screen captures from the clinical ultrasound scanner illustrate (B) non-linear imaging of a tumor showing contrast enhancement before sonoporation, followed by (C) focused ultrasound triggered microbubble destruction *in vivo*. (D) Representative time-intensity curve (TIC) from a pancreatic tumor sonoporated for five treatment cycles. MB reperfusion after the initial (300 sec) and the final (630 sec) flash-destruction pulses was fitted to an exponential model and the resultant curves were compared to assess sonoporation-mediated changes in perfusion kinetics (E).

To cultivate pancreatic tumors, an inoculum of 2×10^6 BxPC3 cells was suspended in 100 μL of RPMI culture media and injected into the subcutaneous space above the right kidney of athymic nude mice (Charles River) aged 4-6 weeks. Tumors were allowed to grow for 3 weeks before commencing sonoporation experiments.

D. Focused Ultrasound Application

A plastic focusing lens (focal length = 3 cm) was attached to a commercial handheld therapeutic ultrasound probe (SoundCare Plus, Austin, TX) in order to elevate pressure in the focal zone (1.2 MPa peak negative pressure). A commercial infusion pump (Kent Scientific) was coupled to a proprietary rotating syringe platform (similar to the system devised in [15]), designed to evenly disperse the microbubbles in solution, ensuring that sustained infusions occurred at a fixed concentration throughout the duration of microbubble administration. Pre- and post-sonoporation kinetics were obtained in a single 10-minute infusion: 1×10^9 microbubbles were combined with 100 μL of DiD-labeled liposomes and brought up to a total volume of 500 μL with sterile saline. Microbubbles were flowed into the tumor space and allowed to reach steady-state over a period of 5 minutes, after which a flash-destruction pulse ($MI = 1.9$) was applied to clear all bubbles from the imaging plane. Microbubbles were then given 30 seconds to re-circulate, following which tumors were sonoporated (1 MHz, 10% duty cycle, 3 W/cm^2) on/off five times for 5 seconds each. This procedure was repeated for five cycles, interspersed by 30-second gaps to permit replenishment. At the 10.5-minute mark, the tumor was hit with a final flash-destruction pulse. Perfusion recovery curves (following both flash-destruction pulses) of the form $y = A(1 - e^{-\beta t})$ were fit to CPS data for specified regions of interest (ROIs) in a custom LabVIEW software. A measure of the relative blood volume (A) and the rate of reperfusion (β) and was compared pre-treatment and post-treatment in the sonoporated region and an unsonoporated area outside the tumor for each mouse (Figure 1).

III. RESULTS AND DISCUSSION

In order to perform reliable qCEUS imaging, we developed a rotating infusion system [15] to deliver microbubbles concurrently with the drug. Owing to their natural buoyancy, microbubbles tend to rise to the surface of a syringe, creating a non-uniform mixture upon injection. The rotation in our custom-built system resulted in a homogenous microbubble solution, thereby ensuring that a steady concentration of microbubbles was in circulation throughout the sonoporation procedure. Since microbubbles present in the ROI increase the recorded pixel intensity proportionally to their concentration, a constant infusion of well mixed microbubbles was critical to yield consistent and reproducible qCEUS imaging.

To evaluate drug uptake resulting from sonoporation *in vivo*, both nanoparticle accumulation and changes in tissue

morphology were qualitatively considered. As depicted in Figure 2, sonoporation resulted in substantially greater liposomal uptake in matrigel plugs, accompanied by no necrosis. This constitutes a crucial finding as sonoporation is intended to drive increased levels of drug into the tumor without inducing vascular collapse. Since therapeutic agents utilize the vasculature as a physical roadway to reach their target site, inflicting irreversible damage on the vascular endothelium would be detrimental to the goal of depositing large drug payloads into the tumor space.

TIC analysis confirms this histology data; sonoporated sections of pancreatic tumors did not experience a decrease in their level of perfusion as compared to unsonoporated sections of tissue lying outside the tumor boundary (Figure 3A). The relative blood volume within a specified 2D region of interest (ROI) can be gleaned from the TIC by observing the signal enhancement from baseline.

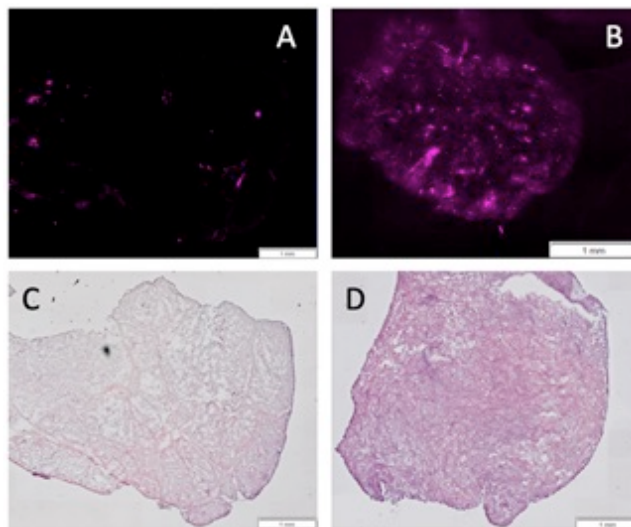


Fig. 2. Evaluating the effects of sonoporation on nanoparticle accumulation. Sections of sonoporated and unsonoporated matrigel plugs co-injected with fluorescently-tagged DiD “mock Doxil” liposomes were visualized on an Olympus VS120 Virtual Slide Microscope at 20X. Improved liposomal uptake was noted in sonoporated samples (B) in comparison with untreated tissue (A), and serial H&E histological staining (C and D) showed no evidence of cell death in either of the treatment groups.

Conversely, the rate of microbubble reperfusion in sonoporated tissue was found to decrease significantly ($p < 0.01$) compared with unsonoporated control tissue. This result is indicative of vascular permeabilization; increased permeability is likely responsible for the enhanced nanoparticle accumulation observed in Figure 2B. We hypothesize that this decline in reperfusion rate can be ascribed to an increase in hematocrit within tumor blood vessels immediately following sonoporation. When vascular endothelial cells are made more permeable by sonoporation, plasma can escape from the tumor vasculature and increase the viscosity of blood, thus increasing resistance to

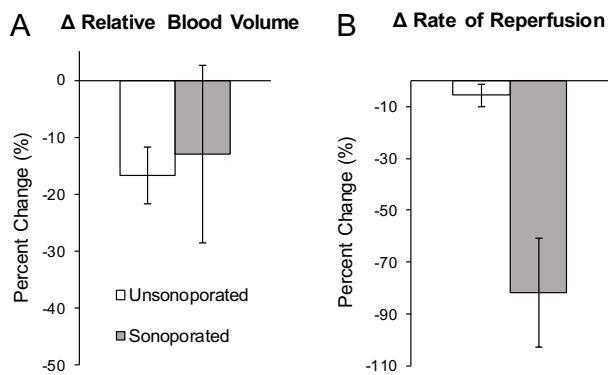


Fig. 3. Quantitative metrics obtained from TIC analysis revealed no significant change in relative blood volume between the unsonoporated (17% decrease) and sonoporated (13% decrease) regions of pancreatic tumors following sonoporation (A), whereas a statistically significant ($*p < 0.01$) decrease in reperfusion rate was observed in the sonoporation focal zone (82% decrease) as compared to the unsonoporated (6% decrease) area (B) which was designated as an internal control of sorts. An unpaired, two-tailed student t-test was performed with $n = 3$ mice per group.

microbubble flow. This leads to a noticeable decrease in the rate at which microbubbles can repopulate the tumor space after an US flash-destruction pulse is applied (Fig. 1D-E). The physical effect sonoporation has on microbubble perfusion kinetics renders it an effective predictor of intratumoral drug uptake, and by extension, sonoporation efficiency as a whole.

IV. CONCLUSION

We have shown that changes in perfusion kinetics can be effective predictors of sonoporation efficiency *in vivo*. More specifically, our data indicates that reperfusion rates may be a better predictor of efficacy than relative blood volume. We plan to extend this line of work by continuing to link perfusion parameters with biological effects from *ex vivo* analysis and elucidating their underlying mechanism; monitoring changes in microvasculature and quantifying the spatial distribution of L-DOX in the tumor are further avenues of exploration that would support our findings. And to further build upon this study, we plan to investigate additional models of cancer. The ultimate goal of this work is to capitalize on the quantitative capacity of CEUS to provide real-time feedback detailing vascular changes that occur during sonoporation, and to eventually relate these biologically driven phenomena with drug uptake. Successful implementation of this strategy is expected to bring about improved methods of monitoring tumor response to therapy in the clinic, and hence, better patient outcomes.

ACKNOWLEDGEMENTS

We would like to thank Kulsoom Javed and Dr. Kenneth Hoyt for providing us with the pancreatic tumor cell line used in the *in vivo* experiments and for assisting with tissue culture prior to tumor implantations.

REFERENCES

- [1] Jain, R. K. & Stylianopoulos, T. Delivering nanomedicine to solid tumors. *Nat. Rev. Clin. Oncol.* **7**, 653–664 (2010).
- [2] Noguchi, Y. *et al.* Early Phase Tumor Accumulation of Macromolecules: A Great Difference in Clearance Rate between Tumor and Normal Tissues. *Jpn. J. Cancer Res.* **89**, 307–314 (1998).
- [3] Prabhakar, U. *et al.* Challenges and Key Considerations of the Enhanced Permeability and Retention Effect for Nanomedicine Drug Delivery in Oncology. *Cancer Res.* **73**, 2412–2417 (2013).
- [4] Bertrand, N., Wu, J., Xu, X., Kamaly, N. & Farokhzad, O. C. Cancer nanotechnology: The impact of passive and active targeting in the era of modern cancer biology. *Adv. Drug Deliv. Rev.* **66**, 2–25 (2014).
- [5] Lammers, T., Kiessling, F., Hennink, W. E. & Storm, G. Drug targeting to tumors: Principles, pitfalls and (pre-) clinical progress. *J. Controlled Release* **161**, 175–187 (2012).
- [6] Taurin, S., Nehoff, H. & Greish, K. Anticancer nanomedicine and tumor vascular permeability: Where is the missing link? *J. Controlled Release* **164**, 265–275 (2012).
- [7] Sirsi, S. R. & Borden, M. A. Microbubble compositions, properties and biomedical applications. *Bubble Sci. Eng. Technol.* **1**, 3–17 (2009).
- [8] Sboros, V. Response of contrast agents to ultrasound. *Adv. Drug Deliv. Rev.* **60**, 1117–1136 (2008).
- [9] Lammertink, B. H. A. *et al.* Sonochemotherapy: from bench to bedside. *Front. Pharmacol.* **6**, (2015).
- [10] Böhmer, M. R. *et al.* Ultrasound triggered image-guided drug delivery. *Eur. J. Radiol.* **70**, 242–253 (2009).
- [11] Theek, B. *et al.* Sonoporation enhances liposome accumulation and penetration in tumors with low EPR. *J. Controlled Release* **231**, 77–85 (2016).
- [12] Tinkov, S. *et al.* New doxorubicin-loaded phospholipid microbubbles for targeted tumor therapy: In-vivo characterization. *J. Controlled Release* **148**, 368–372 (2010).
- [13] Lin, C.-Y., Li, J.-R., Tseng, H.-C., Wu, M.-F. & Lin, W.-L. Enhancement of focused ultrasound with microbubbles on the treatments of anticancer nanodrug in mouse tumors. *Nanomedicine Nanotechnol. Biol. Med.* **8**, 900–907 (2012).
- [14] Wu, S.-Y. *et al.* Transcranial cavitation detection in primates during blood-brain barrier opening—a performance assessment study. *IEEE Trans. Ultrason. Ferroelectr. Freq. Control* **61**, 966–978 (2014).
- [15] Kaya, M., Gregory V, T. S. & Dayton, P. A. Changes in Lipid-Encapsulated Microbubble Population During Continuous Infusion and Methods to Maintain Consistency. *Ultrasound in Medicine & Biology* **35**, 1748–1755 (2009).